International Journal of Remote Sensing
Vol. 28, No. 10, 20 May 2007, 2207–2219

Simulation of vertical wind profile under neutral conditions

T. X. YUE*, W. WANG, Q. YU, Z. L. ZHU, S. H. ZHANG, R. H. ZHANG and Z. P. DU

Institute of Geographical Sciences and Natural Resources Research, Chinese Academy of Sciences, A11, Datun Road, Anwai, 100101 Beijing, PR China

(*Received 26 September 2005; in final form 21 August 2006*)

After analysing formulations of the horizontal wind velocity above a non-uniform underlying surface, it is found that the mean height of roughness elements, fractional vegetation cover and leaf area index are the most essential parameters of vertical wind profile under neutral conditions. By using Landsat-5 data, every-10-days observed data in the field, the every-10-days Normalized Difference Vegetation Index (NDVI) data from NOAA-14 meteorological satellite, 1 : 10 000 land-use data, and 1 : 10 000 topographical data, the mean height, leaf area index and fractional vegetation cover of wheat at Yucheng Integrated Agricultural Experiment Station are simulated as functions of NDVI. Then, hourly horizontal wind velocity at a height of 4 m during the period from 21:05 on 5 March 2000 to 7:05 on 24 May 2000 is calculated, for which hourly observed horizontal wind velocity at a height of 2 m is first used to simulate the wheat parameter of the dimensionless constant. The results show that the simulated velocity is almost identical to the observation velocity at a height of 4 m.

1. Introduction

Wind plays an important role in ecosystem changes. Wind is the dominant disturbance to patterns of vegetation recovery (Schumacher *et al.* 2004). Many herbaceous species rely on wind as their most important dispersal vector (Schippers and Jongejans 2005). Wind is also one of the major dynamic factors that cause extensive damage to ecosystems (Beinhauer and Kruse 1994, Gardiner *et al.* 2000, Blennow and Sallnäs 2004). This paper focuses on simulation of the horizontal wind velocity above a non-uniform underlying surface.

Under thermally neutral conditions, steady-state flow over horizontally bare soil can be described by the well known logarithmic law (Sutton 1953, Mihailovic *et al.* 1999, Baldauf and Fiedler 2003)

$$u(z) = \frac{u_*}{k} \ln \frac{z}{z_0} \tag{1}$$

where $u(z)$ is the horizontal velocity at height z; u_* is the friction velocity for a bare soil, which physically represents the shear stress $\tau = \rho u_*^2$, where ρ is the air density; k is the von Karman's constant taken to be 0.41; and z_0 is the roughness length of a bare soil.

*Corresponding author. Email: yue@lreis.ac.cn

International Journal of Remote Sensing
ISSN 0143-1161 print/ISSN 1366-5901 online
http://www.tandf.co.uk/journals
DOI: 10.1080/01431160600975303

The popular saying (Wieringa 1993) 'z_0 is the height at which the wind speed becomes zero' is therefore true in a purely algebraic sense only according to equation (1). Research results from Blackadar and Tennekes (1968) show that the logarithmic wind profile was not a feature of the lower few metres over homogeneous terrain only, but rather was a consistent description of any surface layer wind field up to heights of 30 m to 100 m. Consequently, the roughness length z_0 is the optimal parameter for specifying terrain effects on wind (Wieringa 1981).

For vegetative surfaces (Sutton 1953)

$$u(z) = \frac{u_*}{k} \ln \frac{z-d}{z_0} \tag{2}$$

where u_* is the friction velocity over the vegetation surface; d is a zero-plane displacement, which is the mean height of the vegetation on which the bulk aerodynamic drag acts; and z_0 is the roughness length. According to this expression, the wind speed is zero at height $d+z_0$, but the logarithmic profile cannot be extrapolated that far downwards. When the quantities d and z_0 are known, the whole profile above a vegetative surface as well as the ratio $\frac{u_*}{k}$ can be obtained if the wind at a single level is known.

Apparently, transfer of momentum between short grass and the atmosphere does not differ so much from the corresponding exchange when bare soil is the underlying surface (Mihailovic *et al.* 1999). Over tall grass, the transfer of momentum into the atmosphere is more intensive since u_* becomes greater than u_{*g}. The difference in these velocity scales physically is from a displacement effect and an increase in z_0.

Equation (2) is not valid when height z is between the height of the vegetation h and some height z^* representing the lower limit of inertial sublayer. Its order of magnitude can vary between $z^*=d+10z_0$ and $z^*=d+20z_0$ (De Bruin and Moore 1985). Since z_0 is around 10% of the canopy height then the thickness of the roughness sublayer can vary between one and two canopy heights. In models of biosphere–atmosphere exchange, when the underlying vegetative surface consists of patches of bare soil and plant communities with different morphological parameters, the level of inhomogeneity in the cover has to be taken into account in addition to a spatially varying displacement height (Mihailovic *et al.* 1999).

Experimental evidence indicates that estimates of momentum transfer coefficient, K_m, above a vegetative surface were 1.5–2.0 times larger than a simple application of equation (2) would indicate. Thus equation (2) can be modified as

$$u(z) = \frac{u_*}{\alpha_G k} \ln \frac{z-d}{z_0} \tag{3}$$

where α_G is a dimensionless constant estimated to be between 1.5 and 2.0 (Raupach and Thom 1981, Massman 1986). Equation (3) can be valid for the lower part of the roughness sublayer only (Mihailovic *et al.* 1999).

Above a non-uniform underlying surface, non-uniformity is expressed by the surface vegetation fractional cover σ, which takes values from 0 when the ground surface is bare soil to 1 when the ground surface is totally covered by plants. Suppose that the underlying surface is a combination of only two homogenous portions characterized by σ and $1-\sigma$, the wind profile can be formulated as (Mihailovic *et al.* 1999)

$$u(z) = \frac{u_*}{k}[\sigma(\alpha-1)+1]^{-1}\ln\frac{[\sigma(\alpha-1)+1]z-\sigma\alpha d}{\alpha^2 z_0} \tag{4}$$

where $u(z)$ is the horizontal velocity at height z; z_0 is the roughness length; u_* is a friction velocity above the non-homogeneous surface; k is the von Karman's constant taken to be 0.41; d is the displacement height, which is the mean height in the vegetation; and α is a dimensionless constant representing a correction to the mixing length in the roughness sublayer.

In terms of equation (4), roughness length z_0, zero-plane displacement height d, dimensionless constant α and vegetation fractional cover σ are the most important parameters of the horizontal velocity $u(z)$.

2. Estimation of the parameters

2.1 *The dimensionless constant α*

Comparing model simulations with observations, Laric (1997) found that for short grass

$$\alpha^2 = (6.4\mathrm{LAI})^{\frac{1}{10}} \tag{5}$$

for tall grass

$$\alpha^2 = (6.4\mathrm{LAI})^{\frac{1}{5}} \tag{6}$$

and for forest

$$\alpha^2 = (3.2\mathrm{LAI})^{\frac{1}{2}} \tag{7}$$

where LAI is leaf area index.

For wheat, as an extension of the dimensionless constants of short grass and tall grass, α is generally expressed as

$$\alpha = (6.4\mathrm{LAI})^{b} \tag{8}$$

where b is the wheat parameter of the dimensionless constant to be simulated.

LAI is the one-side foliage area per ground area ($m^2\,m^{-2}$) (White *et al.* 2000). The simplest and most practical way is to investigate the relationships between LAI and values of various vegetation indices by means of regression models (Asrar *et al.* 1985, Price and Bausch 1995, Wulder 1998, Brown *et al.* 2000, Qi *et al.* 2000, Vaesen *et al.* 2001, Chen *et al.* 2002). These vegetation indices include the simple ratio vegetation index (Nemani *et al.* 1993), the reduced simple ratio vegetation index (Nemani *et al.* 1993), the perpendicular vegetation index (Wiegand and Richardson 1987), the weighted difference vegetation index (Clevers 1989), the normalized difference vegetation index (Goward *et al.* 1985, Yue *et al.* 2002), the soil adjusted vegetation index (Huete 1988), the atmospherically resistant vegetation index (Kaufman and Tanre 1992), the soil and atmospherically resistant vegetation index (Kaufman and Tanre 1992), the modified normalized difference vegetation index (Liu and Huete 1995), and the feedback-based vegetation index (Huete *et al.* 1997). These relationships between LAI and the vegetation indices have the following generalized formulations:

$$\mathrm{LAI} = a\mathrm{VI}^3 + b\mathrm{VI}^2 + c\mathrm{VI} + d \tag{9}$$

$$\mathrm{LAI} = a\mathrm{VI}^b + c \tag{10}$$

$$\mathrm{LAI} = a\ln(b\mathrm{VI} + c) \tag{11}$$

where VI is a vegetation index; a, b, c, and d are empirical parameters and vary with vegetation types.

In addition to the relationships between LAI and vegetation indexes, the LAI-2000 instrument was used in different vegetation types to derive LAI indirectly (Colombo *et al.* 2003, Gower and Norman 1991), i.e.

$$\mathrm{LAI} = -2\int_0^{\frac{\pi}{2}} \ln P(\theta)\cos\theta\sin\theta d\theta \tag{12}$$

where $P(\theta)$ is a gap fraction in five zenith angle θ ranges with midpoints at 7°, 23°, 38°, 53°, and 67°.

2.2 *Vegetation fractional cover σ*

The fractional vegetation cover, the mean vertically projected canopy area per unit ground area is formulated as (Kellerer 1983, Jasinski and Crago 1999)

$$\sigma = 1 - \exp\left\{-\frac{nA_t}{A_p}\right\} \tag{13}$$

where n is the number of roughness elements; A_t is the mean vertically projected canopy area of a single roughness element, A_p is the unit area such as the pixel area.

The fractional vegetation cover, an important element of climate models, was first introduced by Deardorf (1978). Its specification from field-observations has been problematical (Zeng *et al.* 2000). It is a relatively simple parameter to obtain by means of satellite remote sensing, which was mostly formulated as (Baret *et al.* 1995, Wittich and Hansing 1995, Wittich 1997, Gutman and Ignatov 1998, Zeng *et al.* 2000)

$$\sigma(i,j) = 1 - \left(\frac{N_v(i,j) - N(i,j)}{N_v(i,j) - N_s(i,j)}\right)^b \tag{14}$$

or

$$\sigma(i,j) = \frac{N(i,j) - N_s(i,j)}{N_v(i,j) - N_s(i,j) + (1 - d(i,j))(N(i,j) - N_v(i,j))} \tag{15}$$

where $N(i,j) = [\lambda_{NIR}(i,j) - \lambda_{RED}(i,j)]/[\lambda_{NIR}(i,j) + \lambda_{RED}(i,j)]$, $\lambda_{RED}(i, j)$ is the spectral reflectance of the visible red band; $\lambda_{NIR}(i, j)$ is the spectral reflectance of the near-infrared band; $d(i,j) = \left[(\lambda_{NIR}(i,j) + \lambda_{RED}(i,j))_v\right] / \left[(\lambda_{NIR}(i,j) + \lambda_{RED}(i,j))_s\right]$; the subscripts v and s denote values over 100% vegetation cover and bare soil, respectively; b is a parameter to be simulated.

Zeng *et al.* (2000) modified the formulation of fractional vegetation cover so that the fractional vegetation cover is independent of season and represents the annual maximum green vegetation fraction for a given pixel. The modified formulation was expressed as

$$\sigma(i,j) = \frac{N_{\max}(i,j) - N_s(i,j)}{N_v(i,j) - N_s(i,j)} \tag{16}$$

where $N_{\max}(i, j)$ is the annual maximum value of the normalized difference vegetation index $N(i, j)$.

Many other studies (Scanlon *et al.* 2002, Defries *et al.* 1999, 2000) classified the fractional cover into three broad categories: $\sigma_b(i, j)$, a portion of the land surface that always remains as bare soil, $\sigma_w(i, j)$, a portion of the fractional cover that is woody vegetation, and $\sigma_{g/b}(i, j)$, a remaining portion that consists of bare soil and herbaceous vegetation cover. Their relationship is formulated as (Scanlon *et al.* 2002)

$$\langle\sigma_b(i,j)\rangle+\langle\sigma_w(i,j)\rangle+\langle\sigma_{g/b}(i,j)\rangle=1 \tag{17}$$

where <> operator represents spatial averaging; the subscripts b, w and g/b, respectively represent the portion of the land surface that always remains as bare soil, the portion of the fractional cover that is woody vegetation, and the remaining portion that consists of bare soil and herbaceous vegetation cover.

The temporal mean of the observed NDVI at each pixel is equal to the sum of the NDVI weighted by the fractional cover types

$$\overline{N_b}(i,j)\langle\sigma_b(i,j)\rangle+\overline{N_w}(i,j)\langle\sigma_w(i,j)\rangle+\overline{N_{g/b}}(i,j)\langle\sigma_{g/b}(i,j)\rangle=\overline{N}(i,j) \tag{18}$$

where $\overline{\ }$ operator represents temporal averaging; the subscripts b, w and g/b, respectively represent the portion of the land surface that always remains as bare soil, the portion of the fractional cover that is woody vegetation, and the remaining portion that consists of bare soil and herbaceous vegetation cover.

For homogeneous canopies, the relation between fractional vegetation cover and leaf area index was formulated as (Choudhury *et al.* 1994, Baret *et al.* 1995, Wittich 1997)

$$\sigma(i,j)=1-e^{-c\mathrm{LAI}(i,j)} \tag{19}$$

where LAI is leaf area index; c is a constant to be simulated.

2.3 *Roughness length* z_0 *and zero-plane displacement height* d

The most common geometric approach is to use the mean height of roughness elements to estimate zero-plane displacement height d and roughness length z_0 (Grimmond and Oke 1999). The relations between the mean height of roughness elements and d and z_0 are formulated as

$$d=A_dH \tag{20}$$

$$z_0=A_0H \tag{21}$$

where H is the mean height of roughness elements; A_d and A_0 are constants to be simulated.

Garratt's result (1992) showed that A_d=0.67 and A_0=0.10 were good overall mean values for land surfaces. Raupach (1992) noted that for field crops and grass canopies A_d=0.64 and A_0=0.13, for forests A_d=0.8 and A_0=0.06. Jasinski and Crago (1999) compared the various roughness estimates for the Landes Forest (Gash *et al.* 1989, Parlange and Brutsaert 1989, Raupach 1994, Jasinski and Crago 1999) and concluded that A_0 values usually lie between 0.02 and 0.2 and A_d values mostly between 0.6 and 0.9. In dispersion modelling over urban areas,

Hanna and Chang (1992) suggested that A_d=0.5 and A_0=0.10 were useful approximations. Although this parametrization ignores many aspects, it does capture the most important parameter influencing turbulence near the surface and provides a basis for comparisons with more sophisticated models (Yang and Friedl 2003).

A key plant parameter is the frontal area index λ, which is defined as the ratio of frontal area of roughness elements from the mean wind direction per unit ground area. It can be formulated as

$$\lambda = \frac{nA_f}{A_p} \tag{22}$$

where n is the number of roughness elements; A_f is the mean frontal area of an individual roughness element, A_p is the unit area such as the pixel area.

For isotropically oriented elements, the relationship between the frontal area index λ and canopy area index Λ, the total (single-sided) area of all canopy elements over unit ground area, can be formulated as $\Lambda = 2\lambda$. The canopy area index includes all canopy elements, transpiring ones (living leaves and stems) and non-transpiring ones (dead leaves and stems), while leaf area index includes only transpiring surfaces. A_d and A_0 are formulated as (Raupach 1992, 1994)

$$A_d = 1 - \frac{1 - \exp\left(-\sqrt{c_{d1}\Lambda}\right)}{\sqrt{c_{d1}\Lambda}} \tag{23}$$

$$A_0 = (1 - A_d)\exp\left(-k\frac{u_h}{u_*} - \Psi_h\right) \tag{24}$$

where c_{d1} is a free parameter; k is the von Karman's constant; ψ_h is the roughness-sublayer influence function; u_* is the friction velocity; u_h is the mean velocity at height h. When $\lambda \geqslant \lambda_{\max}$, $\frac{u_h}{u_*}$ is nearly constant at 0.3, where $\lambda_{\max}$ is the point at which adding further roughness elements to the surface does not affect the bulk drag because additional elements merely shelter one another. When $\lambda < \lambda_{\max}$, $\frac{u_h}{u_*}$ is the solution of equation

$$\gamma = \frac{u_h}{u_*} = \left(\frac{\exp(\lambda\gamma/4)}{(C_S + C_R\lambda)^{1/2}}\right) \tag{25}$$

where C_S is the drag coefficient of the substrate surface at height h in the absence of roughness elements (about 0.003); C_R is the drag coefficient of an isolated roughness element mounted on the surface.

In addition to the geometric approach and the frontal area index, there have been many well-documented experimental determinations of the roughness over various surfaces, ranging from mobile surfaces (sea, moving sand or snow) to vegetations and towns based on the data of land cover types.

It can be concluded that the mean height of roughness elements (H), fractional vegetation cover (σ) and leaf area index (LAI) are the most essential parameters of the vertical wind profile under neutral conditions. Currently, wind speed models require either field validation of simulated LAI, σ and H, or remotely sensed estimates of LAI, σ and H to initiate them (Running *et al.* 1999). LAI, σ and H measurements are critical for improving the performance of such models over large

areas and this has prompted investigations into the relationship between ground-measured LAI, σ and H and spectral vegetation indexes derived from satellite-measured data (Colombo *et al.* 2003).

3. Simulation of vertical wind profile

3.1 *Retrieval of the essential wheat parameters at Yucheng Integrated Agricultural Experiment Station, Chinese Academy of Sciences, Shandong Province*

In north China, the period from the first 10-days of March to the first 10-days of April is the optimum time for identifying wheat among other crops because wheat is the sole crop that has become green in this period. According to available NDVI data and Landsat TM data from archives, Landsat-5 data on 30 March 2000 are selected to identify wheat land-use type, of which projection is chosen as Albers Conical Equal Area. Observation data in the field and other auxiliary data include: (1) every-10-days observed data of mean height, leaf area index and fractional vegetation cover of the wheat at Yucheng Integrated Agricultural Experiment Station, Chinese Academy of Sciences, Shandong Province (36°49′52″ N, 116°34′17″ E) in 2000 (table 1); (2) the every-10-days NDVI data from NOAA-14 meteorological satellite; (3) 1 : 10 000 land-use data; (4) 1 : 10 000 topographical data.

The data pre-processing includes the following steps: (1) to collect 41 control points on the 1 : 10 000 topographical map and to geometrically correct the Landsat TM image (figure 1); (2) to conduct resampling by means of the proximity-element method in order to easily classify the image and keep the relatively proportional relation of grey gradations of the original image, (3) to create 25 m × 25 m corrected Landsat TM data; (4) to conduct projection transformation of the every-10-days NDVI data from Lambert homolographic projection to Albers Conical homolographic projection; (5) to conduct registration of the every-10-days NDVI data with the 1 : 10 000 land-use map of Yucheng, Shandong province; (6) to fit the original image by means of a quadratic polynomial.

Table 1. Observation values of relative parameters in 2000 (source: Yucheng Integrated Agricultural Experiment Station, Chinese Academy of Sciences, Shandong Province).

Observation date (2000)	Stem height (cm)	Leaf area index	Fractional vegetation cover (%)
5 March	13.5	2.18	20
15 March	21.6	2.58	25
20 March	22.6	3.3	33
25 March	24.2	3.58	36
30 March	29.2	4.58	39
4 April	35.4	4.61	44
9 April	45.4	4.88	50
14 April	55	4.97	62
19 April	73.6	4.98	70
24 April	84.5	5.04	90
29 April	85	4.98	95
4 May	93	3.76	95
9 May	93	3.29	95
14 May	93.2	2.93	90
19 May	93.2	2.38	88
24 May	93.2	1.55	80

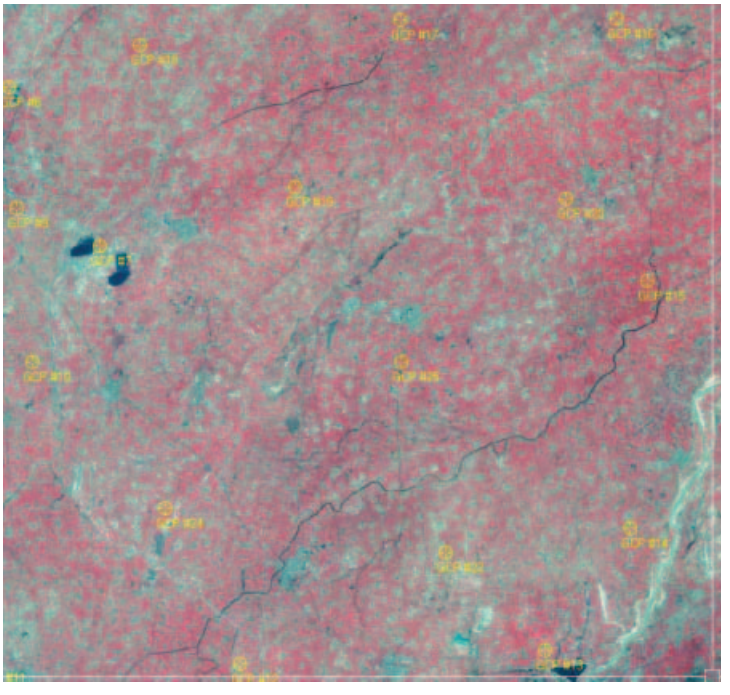

Figure 1. Landsat-5 TM image and control points for geometrical correction.

The simulation results show that

$$\mathrm{LAI}=\begin{cases}-51.915+11.603\ln(NDVI_s) & \text{when } NDVI_s \text{ increases(correlation coefficient is 0.889)}\\ -51.751+11.077\ln(NDVI_s) & \text{when } NDVI_s \text{ decreases(correlation coefficient is 0.860)}\end{cases} \quad (26)$$

$$H=\begin{cases}-238.753+2.251NDVI_s & \text{when } NDVI_s \text{ increases (correlation coefficient is 0.868)}\\ 93.2\,\mathrm{cm} & \text{when } NDVI_s \text{ decreases}\end{cases} \quad (27)$$

$$\sigma=\begin{cases}e^{28.308+5.679\ln(NDVI_s)} & \text{when } NDVI_s \text{ increases(correlation coefficient is 0.920)}\\ e^{-3.712+0.733\ln(NDVI_s)} & \text{when } NDVI_s \text{ increases(correlation coefficient is 0.889)}\end{cases} \quad (28)$$

where $NDVI_s=100(NDVI+1)$; LAI is leaf area index; H is the mean height of wheat; and σ is the fractional vegetation cover.

The scaled NDVI, $NDVI_s$, is derived from NOAA-14 data. $NDVI_s$ increases from early March to early May and decreases from early May to June. $NDVI_s$ ranges from 90 to 160 at Yucheng Integrated Agricultural Experiment Station, Chinese Academy of Sciences in Shandong province.

3.2 *Simulation of horizontal wind velocity above the wheat surface at Yucheng Integrated Agricultural Experiment Station, Chinese Academy of Sciences, Shandong Province*

According to equations (4) and (8) as well as discussions on roughness length and displacement height, horizontal wind velocity at height z and at time t is formulated

as

$$u(z,t)=\frac{2.44u_*(t)}{\sigma(t)\left((6.4\mathrm{LAI}(t))^b-1\right)+1}\ln\frac{\left[\sigma(t)\left((6.4\mathrm{LAI}(t))^b-1\right)+1\right]z-0.64H(t)\sigma(t)(6.4\mathrm{LAI}(t))^b}{(0.13H(t))\left((6.4\mathrm{LAI}(t))^{2b}\right)} \quad (29)$$

where $u_*(t)$ is the friction velocity over the wheat surface; LAI(t) is the leaf area index; $H(t)$ is the mean height of wheat; $\sigma(t)$ is the fractional vegetation cover of wheat; b is the wheat parameter of the dimensionless constant to be simulated.

The simulation result most fits the observation of horizontal wind velocity at a height of 2 m when $b=0.39$ (figure 2). The horizontal wind velocity is expressed as

$$u(z,t)=\frac{2.44u_*(t)}{2.06\sigma(t)(\mathrm{LAI}(t))^{0.39}+(1-\sigma(t))}\ln\frac{\left[2.06\sigma(t)(\mathrm{LAI}(t))^{0.39}+(1-\sigma(t))\right]z-1.32H(t)\sigma(t)(\mathrm{LAI}(t))^{0.39}}{0.55H(t)(\mathrm{LAI}(t))^{0.78}} \quad (30)$$

The hourly horizontal wind velocity at a height of 4 m during the period from 21:05 on 5 March 2000 to 7:05 on 24 May 2000, which is simulated by means of equation (30), is almost identical to the observation ones (figure 3). The correlation coefficient between the simulation results and the observation values is 0.998.

4. Conclusion

Our review of studies on wind profile shows that horizontal wind velocity above a non-uniform underlying surface is determined by roughness length, zero-plane displacement height, dimensionless constant and vegetation fractional cover. Roughness length and zero-plane displacement height can be expressed as a mathematical function of the mean height of roughness elements; the dimensionless constant can be formulated as a function of leaf area index. Therefore, the mean height of roughness elements, fractional vegetation cover and leaf area index are involved in the formulation of horizontal wind velocity as the most essential parameters. The case-study at Yucheng Integrated Agricultural Experiment Station, Chinese Academy of Sciences, Shandong Province shows that the mean height of roughness elements, fractional vegetation cover and leaf area index are closely related to the normalized difference vegetation index (NDVI). They are retrieved

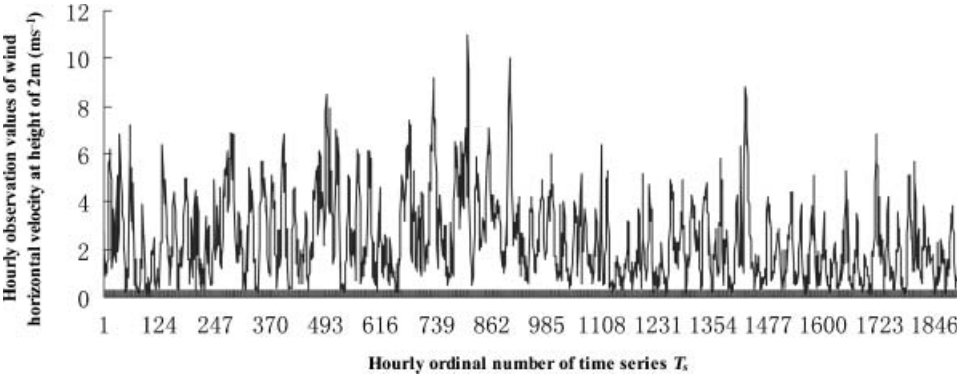

Figure 2. Hourly observation of horizontal wind velocity at height 2 m during the period from 21:05 on 5 March 2000 to 7:05 on 24 May 2003 at Yucheng Integrated Agricultural Experiment Station (when observation time is 21:05 on 5 March 2000, $T_s=1$; when observation time is 7:05 on 24 May 2000, $T_s=1929$).

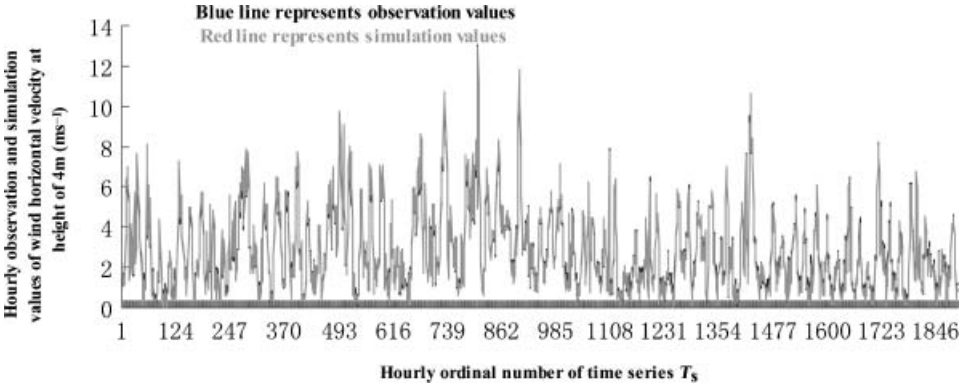

Figure 3. Comparison between hourly observation and the simulation of horizontal wind velocity at a height of 4 m during the period from 21:05 on 5 March 2000 to 7:05 on 24 May 2003 at Yucheng Integrated Agricultural Experiment Station (when observation time is 21:05 on 5th March of 2000, T_s=1; when observation time is 7:05 on 24 May 2000, T_s=1929).

from the scaled NDVI. A model of vertical wind profile (MVWP), the relationship between horizontal wind velocity and NDVI is finally established. The simulated horizontal wind velocity is almost the same as the observed one at the Yucheng Integrated Agricultural Experiment Station, which means that MVWP is applicable to formulate horizontal wind velocity under thermally neutral conditions.

Acknowledgments

This work is supported by the Project of National Natural Science Foundation of China (40371094) and the Fund for Outstanding Overseas Young Scientists of the Chinese Academy of Sciences (2001-01-13).

References

Asrar, G., Kanemasu, E.T. and Yoshida, M., 1985, Estimates of leaf area index from spectral reflectance of wheat under different cultural practices and solar angle. *Remote Sensing of Environment*, **17**, pp. 1–11.

Baldauf, M. and Fiedler, F., 2003, A parameterisation of the effective roughness length over inhomogenous, plat terrain. *Boundary-Layer Meteorology*, **106**, pp. 189–216.

Baret, F., Clevers, J.G.P.W. and Steven, M.D., 1995, The robustness of canopy gap fraction estimates from red and near-infrared reflectances: a comparison of approaches. *Remote Sensing of Environment*, **54**, pp. 141–151.

Beinhauer, R. and Kruse, B., 1994, Soil erosivity by wind in moderate climates. *Ecological Modelling*, **75/76**, pp. 279–287.

Blackadar, A.K. and Tennekes, H., 1968, Asymptotic similarity in neutral barotropic planetary boundary layers. *Journal of the Atmospheric Sciences*, **25**, pp. 1015–1020.

Blennow, K. and Sallnäs, O., 2004, WINDA—a system of models for assessing the probability of wind damage to forest stands within a landscape. *Ecological Modelling*, **175**, pp. 87–99.

Brown, L.J., Chen, J.M., Leblance, S.G. and Cihlar, J., 2000, A shortwave infrared modification to the simple ratio for LAI retrieval in boreal forests: an image and model analysis. *Remote Sensing of Environment*, **71**, pp. 16–25.

Chen, J.M., Pavlic, G., Brown, L., Cihlar, J., Leblance, S.G., White, H.P., Hall, R.J., Peddle, D.R., King, D.J., Trofymow, J.A., Swift, E., van der sanden, J. and Pellikka, P.K.E., 2002, Derivation and validation of Canada-wide coarse-resolution leaf area index maps using high-resolution satellite imagery and ground measurements. *Remote Sensing of Environment*, **80**, pp. 165–184.

CHOUDHURY, B.J., AHMED, N.U., IDSO, S.B., REGINATO, R.J. and DAUGHTRY, C.S.T., 1994, Relations between evaporation coefficients and vegetation indexes studied by model simulation. *Remote Sensing of Environment*, **50**, pp. 1–17.

CLEVERS, J.G.P.W., 1989, The application of a weighted infrared-red vegetation index for estimating leaf area index by correcting for soil moisture. *Remote Sensing of Environment*, **29**, pp. 25–37.

COLOMBO, R., BELLINGERI, D., FASOLINI, H. and MARINO, C.M., 2003, Retrieval of leaf area index in different vegetation types using high resolution satellite data. *Remote Sensing of Environment*, **86**, pp. 120–131.

DEARDORFF, J.W., 1978, Efficient prediction of ground temperature and moisture with inclusion of a layer of vegetation. *Journal of Geophysical Research*, **83**, pp. 1889–1903.

DE BRUIN, H.A.R. and MOORE, C.J., 1985, Zero-plane displacement and roughness length for tall vegetation, derived from a simple mass conservation hypothesis. *Boundary-Layer Meteorology*, **42**, pp. 53–62.

DEFRIES, R.S., TOWNSHEND, J.R.G. and HANSEN, M.C., 1999, Continuous fields of vegetation characteristics at the global scale. *Journal of Geophysical Research*, **104**, pp. 16911–16923.

DEFRIES, R.S., HANSEN, M.C. and TOWNSHEND, J.R.G., 2000, Global continuous fields of vegetation characteristics: a linear mixture applied to multi-year 8 km AVHRR data. *International Journal of Remote Sensing*, **21**, pp. 1389–1414.

DEFRIES, R.S., HANSEN, M.C., TOWNSHEND, J.R.G., JANETOS, A.C. and LOVELAND, T.R., 2000, A new global 1-km dataset of percentage tree cover derived from remote sensing. *Global Change Biology*, **6**, pp. 247–254.

GARDINER, B., PELTOLA, H. and KELLOMÄKI, S., 2000, Comparison of two models for predicting the critical wind speeds required to damage coniferous trees. *Ecological Modelling*, **129**, pp. 1–23.

GARRATT, J.R., 1992, *The Atmospheric Boundary Layer* (London: Cambridge University Press).

GASH, J.H., SHUTTLEWORTH, W.J. and LLOYD, C.R., 1989, Micrometeorological measurements in Les Landes Forest during HAPEX-Mobilhy. *Agricultural and Forest Meteorology*, **46**, pp. 131–147.

GOWARD, S.N., TUCKER, C.J. and DYE, D.G., 1985, North American vegetation patterns observed with NOAA-AVHRR. *Vegetation*, **64**, pp. 3–14.

GOWER, S.T. and NORMAN, J.M., 1991, Rapid estimation of leaf area index for forests using LI-COR LAI-2000. *Ecology*, **72**, pp. 1896–1900.

GRIMMOND, C.S.B. and OKE, T.R., 1999, Aerodynamic properties of urban areas derived from analysis of surface form. *Journal of Applied Meteorology*, **38**, pp. 1262–1292.

GUTMAN, G. and IGNATOV, A., 1998, The derivation of the green vegetation fraction from NOAA/AVHRR data for use in numerical weather prediction models. *International Journal of Remote Sensing*, **19**, pp. 1533–1543.

HANNA, S.R. and CHANG, J.C., 1992, Boundary layer parameterizations for applied dispersion modelling over urban areas. *Boundary-Layer Meteorology*, **58**, pp. 229–259.

HUETE, A.R., 1988, A soil adjusted vegetation index (SAVI). *Remote Sensing of Environment*, **25**, pp. 295–309.

HUETE, A.R., LIU, H.Q., BATCHILY, K. and VAN LEEUWEN, W., 1997, A comparison of vegetation indices over a global set of TM images from EOS-MODIS. *Remote Sensing of Environment*, **59**, pp. 440–451.

JASINSKI, M.F. and CRAGO, R.D., 1999, Estimation of vegetation aerodynamic roughness of natural regions using frontal area density determined from satellite imagery. *Agricultural and Forest Meteorology*, **94**, pp. 65–77.

KAUFMAN, Y.J. and TANRE, D., 1992, Atmospherically resistant vegetation index (ARVI) for EOS-MODIS. IEEE Transactions on *Geoscience and Remote Sensing*, **30**, pp. 261–270.

KELLLERER, A.M., 1983, On the number of clumps resulting from the overlap of randomly placed figures in a plane. *Journal of Applied Probability*, **20**, pp. 126–135.

LARIC, B., 1997, Profile of Wind Speed in Transition Layer above the Vegetation. MSc thesis, University of Belgrade.

LIU, H.Q. and HUETE, A.R., 1995, A feedback based modification of the NDVI to minimize canopy background and atmospheric noise. *IEEE Transactions on Geoscience and Remote Sensing*, **33**, pp. 457–465.

MASSMAN, W., 1986, A comparative study of some mathematical models of the mean wind structure and aerodynamic drag of plant canopies. *Boundary-Layer Meteorology*, **40**, pp. 179–197.

MIHAILOVIC, D.T., LALIC, B., RAJKOVIC, B. and ARSENIC, I., 1999, A roughness sublayer wind profile above a non-uniform surface. *Boundary-Layer Meteorology*, **93**, pp. 425–451.

NEMANI, R., PIERCE, L., RUNNING, S.W. and BAND, L., 1993, Forest ecosystem processes at the watershed scale: sensitivity to remotely sensed leaf area index estimates. *International Journal of Remote Sensing*, **14**, pp. 2519–2534.

PARLANGE, M.R. and BRUTSAERT, W., 1989, Regional roughness of the Landes Forest and surface shear stress under neutral conditions. *Boundary-Layer Meteorology*, **48**, pp. 69–76.

PRICE, J.C. and BAUSCH, J.G., 1995, Leaf area index estimation from visible and near-infrared reflectance data. *Remote Sensing of Environment*, **52**, pp. 55–65.

QI, J., KERR, Y.H., MORAN, M.S., WELTZ, M., HUETE, A.R., SOROOSHIAN, S. and BRYANT, R., 2000, Leaf area index estimates using remotely sensed data and BRDF models in a semiarid region. *Remote Sensing of Environment*, **73**, pp. 18–30.

RAUPACH, M.R., 1992, Drag and drag partition on rough surface. *Boundary-Layer Meteorology*, **60**, pp. 375–395.

RAUPACH, M.R., 1994, Simplified expressions for vegetation roughness length and zero-plane displacement as functions of canopy height and area index. *Boundary-Layer Meteorology*, **71**, pp. 211–216.

RAUPACH, M.R. and THOM, A.S., 1981, Turbulence in and above plant canopies. *Annual Review of Fluid Mechanics*, **13**, pp. 97–129.

RUNNING, S.W., BALDOCCHI, D.D., TURNER, D.P., GOWER, S.T., BAKWIN, P.S. and HIBBARD, K.A., 1999, A global terrestrial monitoring network integrating tower fluxes, flash sampling, ecosystem modeling and EOS satellite data. *Remote Sensing of Environment*, **70**, pp. 108–127.

SCANLON, T.M., ALBERTSON, J.D., CAYLOR, K.K. and WILLIAMS, C.A., 2002, Determining land surface fractional cover from NDVI and rainfall time series for a savanna ecosystem. *Remote Sensing of Environment*, **82**, pp. 376–388.

SCHIPPERS, P. and JONGEJANS, E., 2005, Release thresholds strongly determine the range of seed dispersal by wind. *Ecological Modelling*, **185**, pp. 93–103.

SCHUMACHER, S., BUGMANN, H. and MLADENOFF, D.J., 2004, Improving the formulation of tree growth and succession in a spatially explicit landscape model. *Ecological Modelling*, **181**, pp. 175–194.

SUTTON, O.G., 1953, *Micrometeorology* (New York: McGraw-Hill).

VAESEN, K., GILLIAMS, S., NACKAERTS, K. and COPPIN, P., 2001, Ground-measured spectral signatures as indicators of ground cover and leaf area index: the case of paddy rice. *Field Crops Research*, **69**, pp. 13–25.

WHITE, M.A., ASNER, C.P., NEMANI, R.R., PRIVETTE, J.L. and RUNNING, S.W., 2000, Measuring fractional cover and leaf area index in arid ecosystems: digital camera, radiation transmittance, and laser altimetry methods. *Remote Sensing of Environment*, **74**, pp. 45–57.

WIEGAND, C.L. and RICHARDSON, A.J., 1987, Spectral components analysis: rationale and results for three crops. *International Journal of Remote Sensing*, **8**, pp. 1011–1032.

WIERINGA, J., 1981, Estimation of meso-scale and local-scale roughness for atospheric transport modeling. In *Air Pollution Modeling and Its Application*, C. de Wispelaere, (Ed), pp. 279–295 (New York: Plenum).

WIERINGA, J., 1993, Representative roughness parameters for homogeneous terrain. *Boundary Layer Meteorology*, **63**, pp. 323–363.

WITTICH, K.P., 1997, Some simple relationships between land-surface emissivity, greenness and the plant cover fraction for use in satellite remote sensing. *International Journal of Biometeorology*, **41**, pp. 58–64.

WITTICH, K.P. and HANSING, O., 1995, Area-averaged vegetative cover fraction estimated from satellite data. *International Journal of Biometeorology*, **38**, pp. 209–215.

WULDER, M.A., 1998, The prediction of leaf area index from forest polygons decomposed through the integration of remote sensing, GIS, UNIX, and C. *Computer and Geosciences*, **24**, pp. 151–157.

YANG, R.Q. and FRIEDL, M.A., 2003, Determination of roughness length for heat and momentum over boreal forests. *Boundary-Layer Meteorology*, **107**, pp. 581–603.

YUE, T.X., CHEN, S.P., XU, B., LIU, Q.S., LI, H.G., LIU, G.H. and YE, Q.H., 2002, A curve-theorem based approach for change detection and its application to Yellow River delta. *International Journal of Remote Sensing*, **23**, pp. 2283–2292.

ZENG, X., DICKINSON, R.E., WALKER, A., SHAIKH, M., DEFRIES, R.S. and QI, J., 2000, Derivation and evaluation of global 1-km fractional vegetation cover data for land modeling. *Journal of Applied Meteorology*, **39**, pp. 826–839.